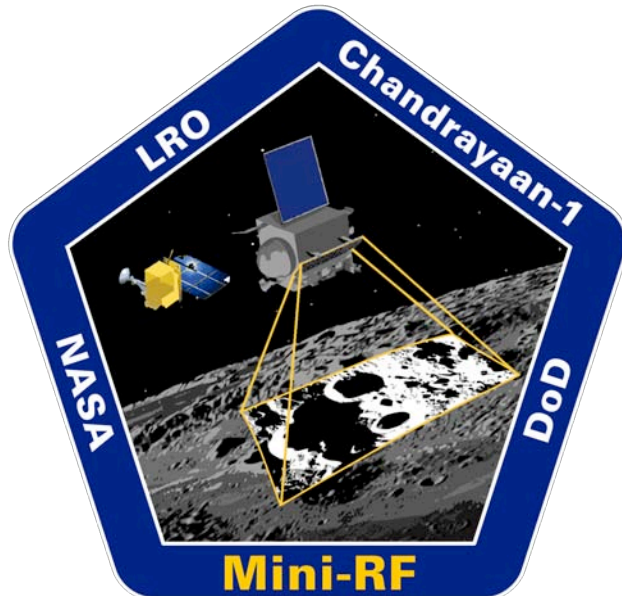




Mini-SAR

Results from Calibration, Mapping, and Analysis



P. D. Spudis, Lunar and Planetary Institute, Houston TX
D.B.J. Bussey, Applied Physics Laboratory, Laurel MD
S. Baloga, Proxemy Research Inc.
B. Butler, National Radio Astronomy Observatory, Socorro NM
L. Carter, National Air and Space Museum, Washington DC
M. Chakraborty, Space Applications Centre, ISRO, Ahmedabad India
J. Gillis-Davis, University of Hawaii, Honolulu HI
J. Goswami, Physical Research Laboratory, Ahmedabad India
E. Heggy, Jet Propulsion Laboratory, Pasadena CA
R. Kirk, U. S. Geological Survey, Flagstaff AZ
C. Neish, Applied Physics Laboratory, Laurel MD
S. Nozette, Lunar and Planetary Institute, Houston TX
M. Robinson, Arizona State University, Tempe AZ
R. K. Raney, Applied Physics Laboratory, Laurel MD
T. Thompson, Jet Propulsion Laboratory, Pasadena CA
B. Thomson, Applied Physics Laboratory, Laurel MD
E. Ustinov, Jet Propulsion Laboratory, Pasadena CA

NLSI Lunar Science Forum

21 July, 2010



The search for lunar ice

"To be uncertain is uncomfortable but to be certain is ridiculous." – Goethe

Radar has been used since 1960's
to map the lunar surface

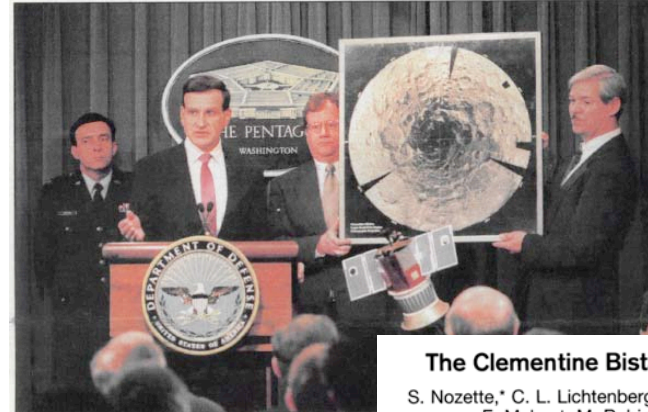
Backscattering properties are
different for normal Moon and
water ice

Long recognized that polar areas
are dark and cold (Watson,
Murray and Brown, 1961)

Discovery of ice at poles of Mercury
in 1992 spurred renewed
interest in lunar poles

Unfavorable viewing geometry
complicated the interpretation of
results

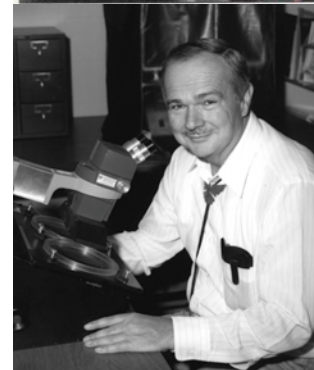
Thus, 20 years of controversy



The Clementine Bistatic Radar Experiment

S. Nozette,* C. L. Lichtenberg, P. Spudis, R. Bonner, W. Ort,
E. Malaret, M. Robinson, E. M. Shoemaker

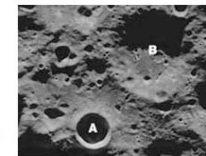
During the Clementine 1 mission, a bistatic radar experiment measured the magnitude and polarization of the radar echo versus bistatic angle, β , for selected lunar areas. Observations of the lunar south pole yield a same-sense polarization enhancement around $\beta = 0$. Analysis shows that the observed enhancement is localized to the permanently shadowed regions of the lunar south pole. Radar observations of periodically solar-illuminated lunar surfaces, including the north pole, yielded no such enhancement. A probable explanation for these differences is the presence of low-loss volume scatterers, such as water ice, in the permanently shadowed region at the south pole.



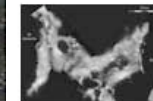
Ice Store At Moon's South Pole Is A Myth

by Staff Writers
Paris (AFP) Oct 18, 2006

Hopes that the Moon's South Pole has a vast hoard of ice that could be used to establish a lunar colony are sadly unfounded, a new study says. In 1994, radar echoes sent back in an experiment involving a US orbiter called Clementine appeared to show that a treasure trove of frozen water lay below the dust in craters near the lunar South Pole that were permanently shaded from the Sun.



Because of the tilt of the moon's orbital plane relative to the Earth's equatorial plane, the Earth can rise much higher above the



Water on the Moon? Scientists Await Definitive Answer

By Rick Callahan

Associated Press
posted: 01:00 pm ET
12 November 2003





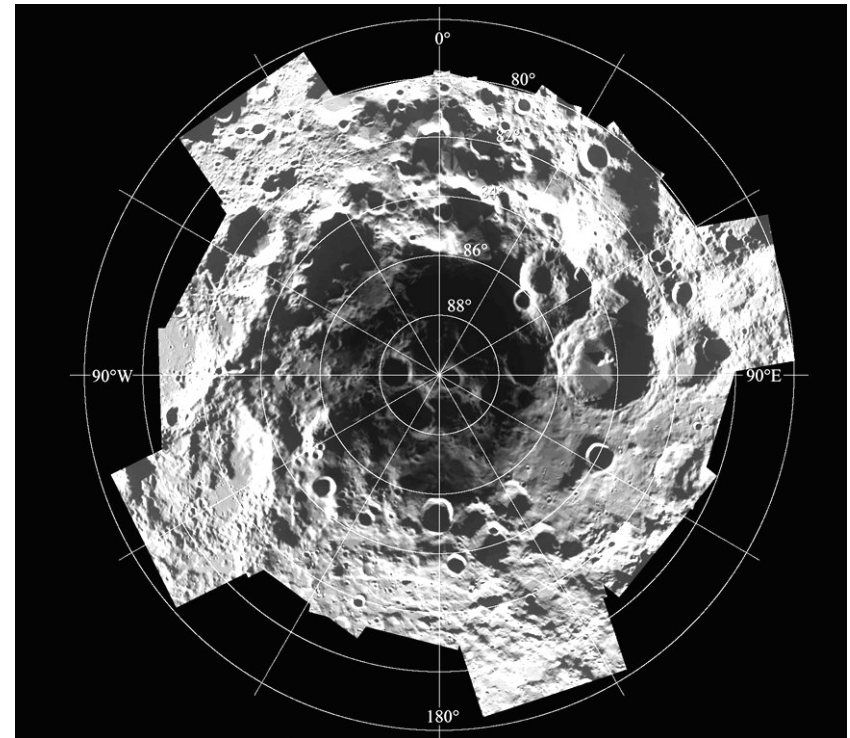
Mini-SAR Experiment Objectives

Map the deposits of both poles of the Moon ($> 80^\circ$ lat.) at optimum viewing angles ($\sim 40^\circ$) to characterize permanently dark areas and definitively determine their RF backscattering properties using both SAR and scatterometry

Complete the global map of the Moon by mapping dark regions in lunar polar areas

Characterize the physical nature of the polar regolith and surface

SAR mapping of other targets of opportunity as possible



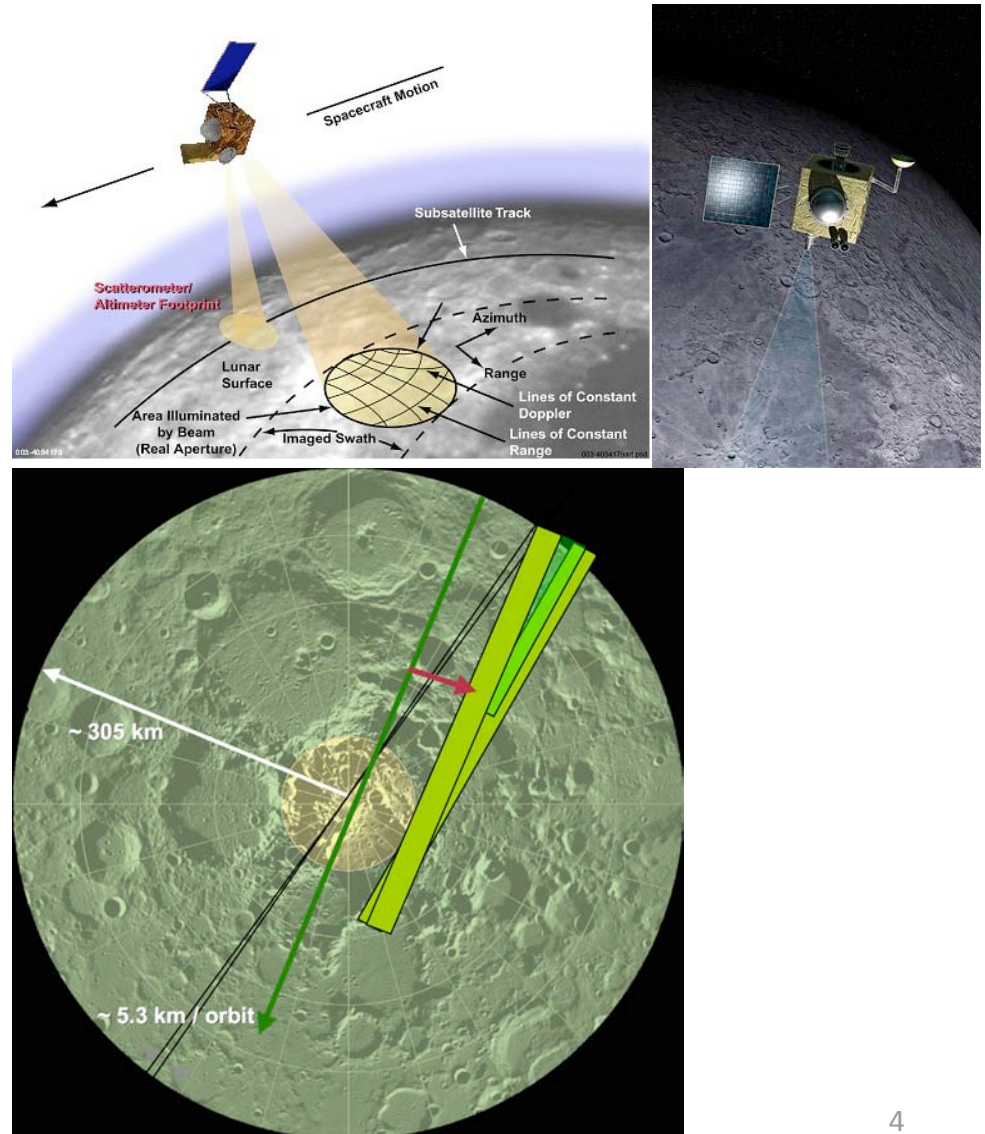
Moon South Pole
Clementine 750 nm base map



Mini-SAR

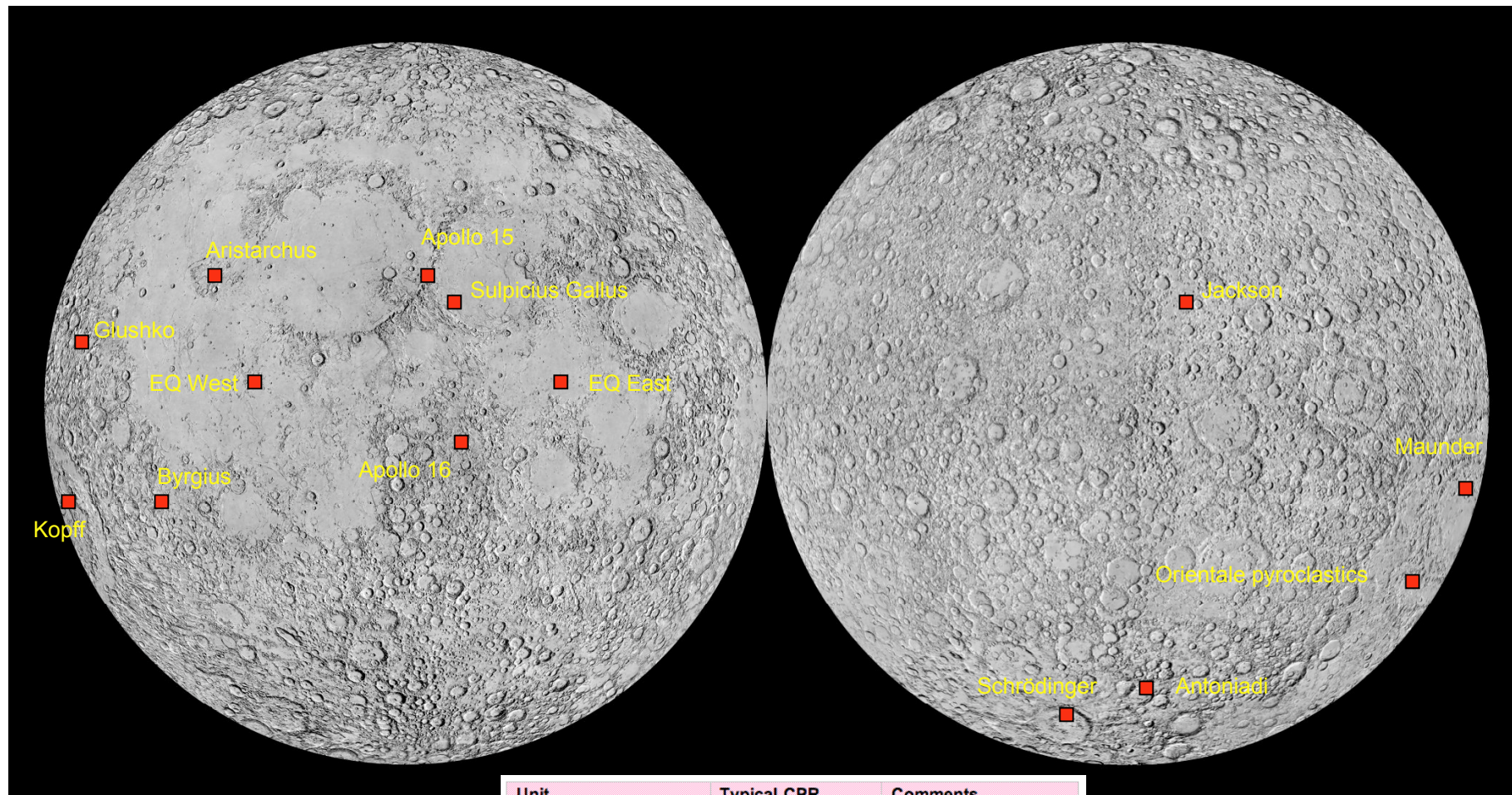
Imaging Radar on the Chandrayaan-1

- Mini-SAR is an S-band (13 cm) imaging radar with hybrid polarity architecture
- Map both polar regions at 75 m/pixel
- Transmit LCP, receive **H** and **V** linear, coherently
- Use Stokes parameters and derived “daughter” products to describe backscattered field
- Map locations and extent of anomalous radar reflectivity
- See polar dark areas (not visible from Earth)
- Cross-correlate with other data sets (topography, thermal, neutron)
- LRO version (Mini-RF) has two bands ($\lambda=13$ and 5 cm), high-resolution zoom mode (15 m/pixel)





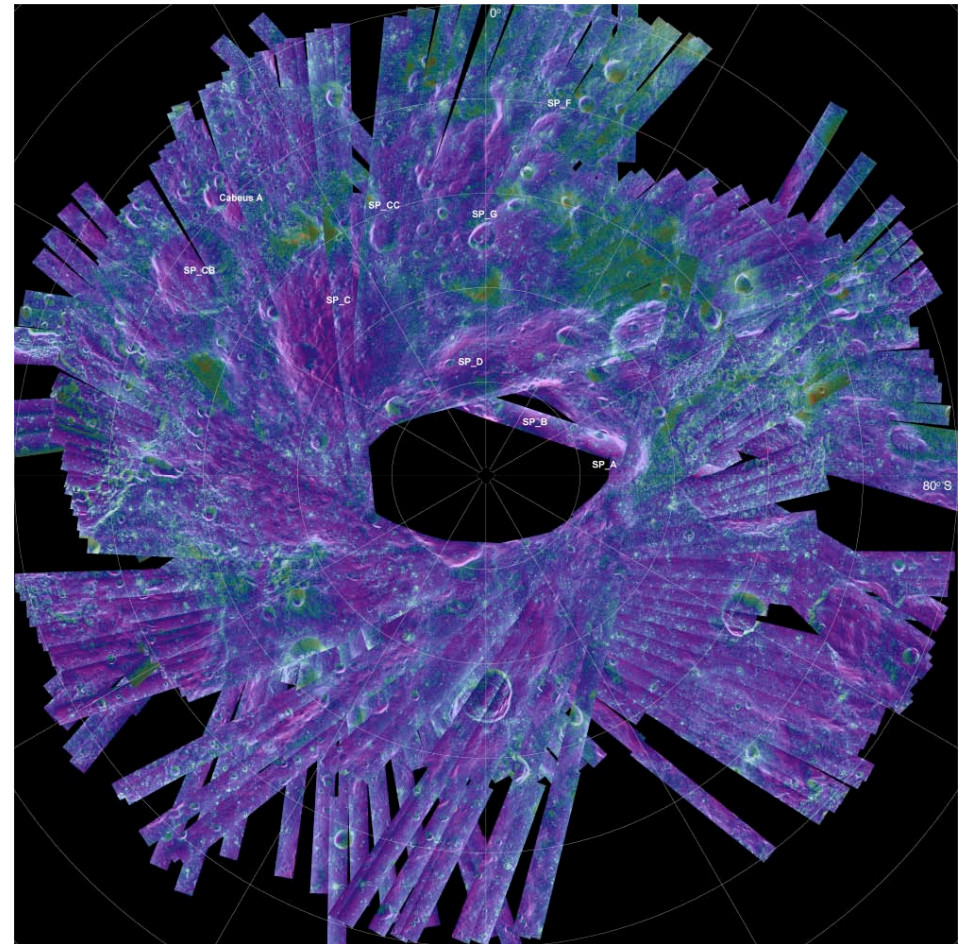
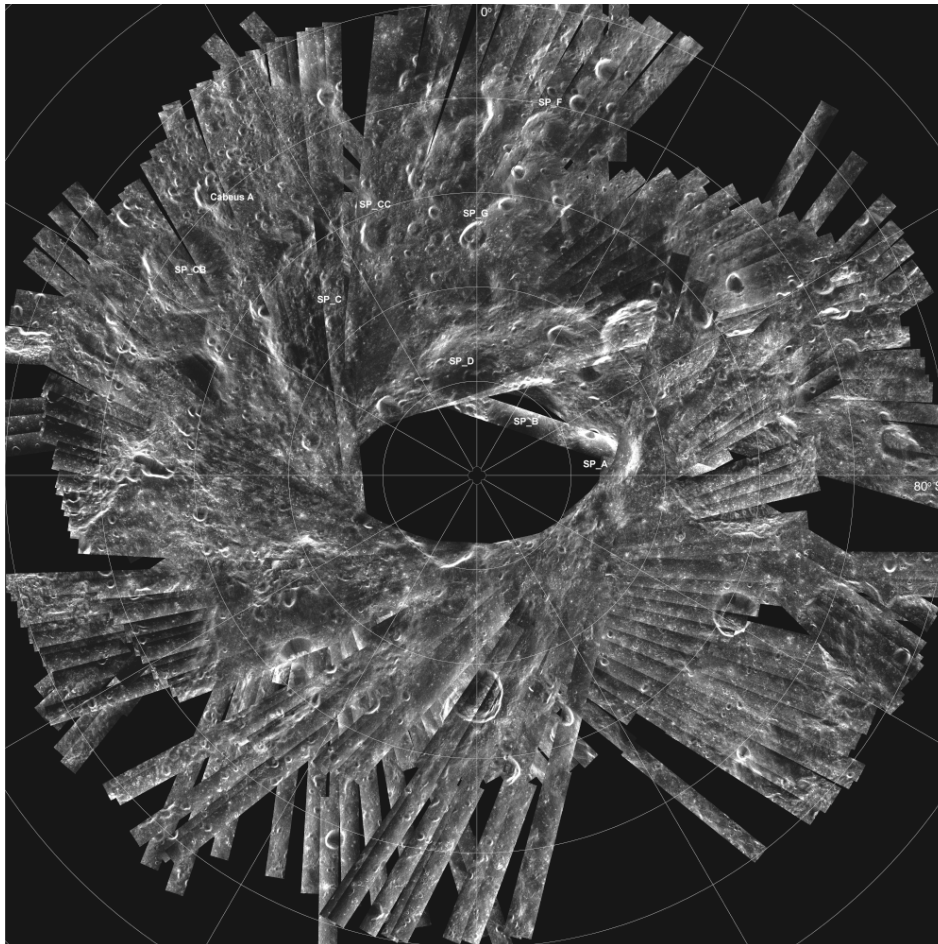
MSR non-polar targets



| Unit | Typical CPR | Comments |
|--------------------------------------------|-------------------|--------------------|
| Aristarchus (Copernican-age crater ejecta) | 0.469 ± 0.149 | Large fresh crater |
| Aratus (Copernican) | 0.743 ± 0.239 | Small fresh crater |
| Apollo 16 Cayley Fm. | 0.311 ± 0.084 | Highland plains |
| Apennine massif | 0.713 ± 0.244 | Mt. Hadley |
| Apennine intermontane | 0.338 ± 0.128 | Apennine backslope |
| "Young" maria | 0.321 ± 0.113 | West of Lansberg |
| Sulpicius Gallus Fm. dark mantle deposits | 0.179 ± 0.055 | Near vent |

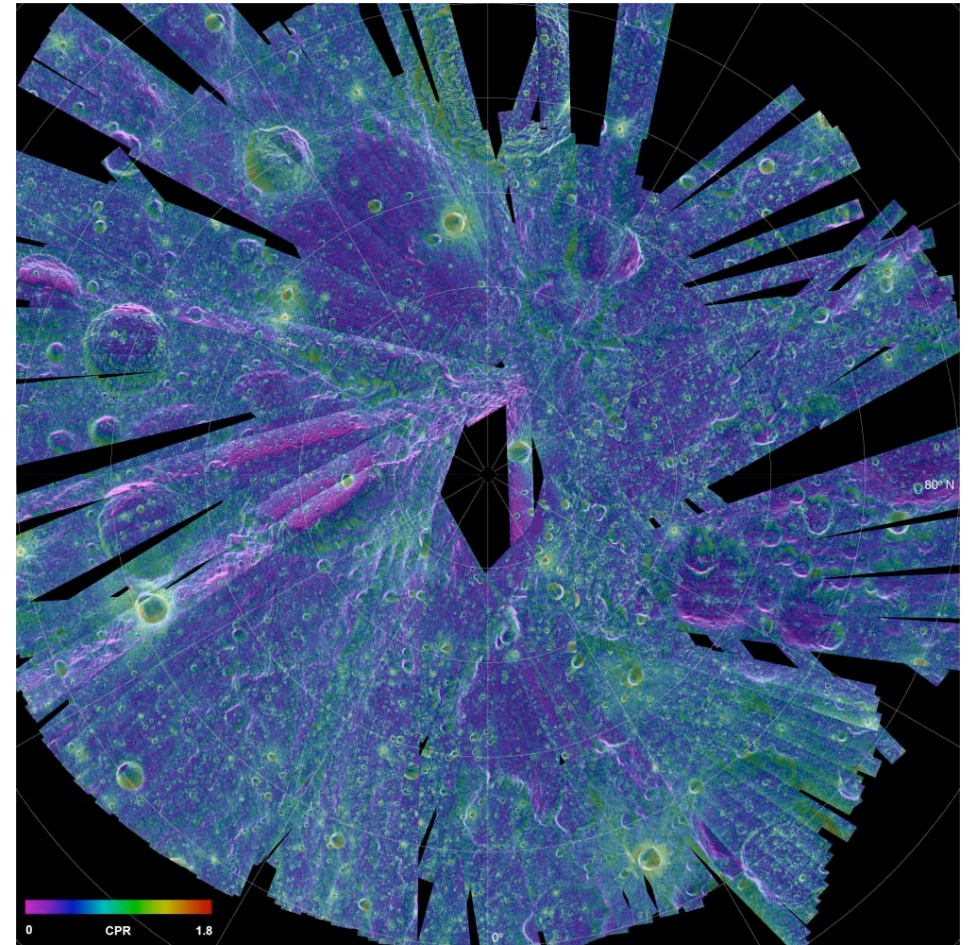
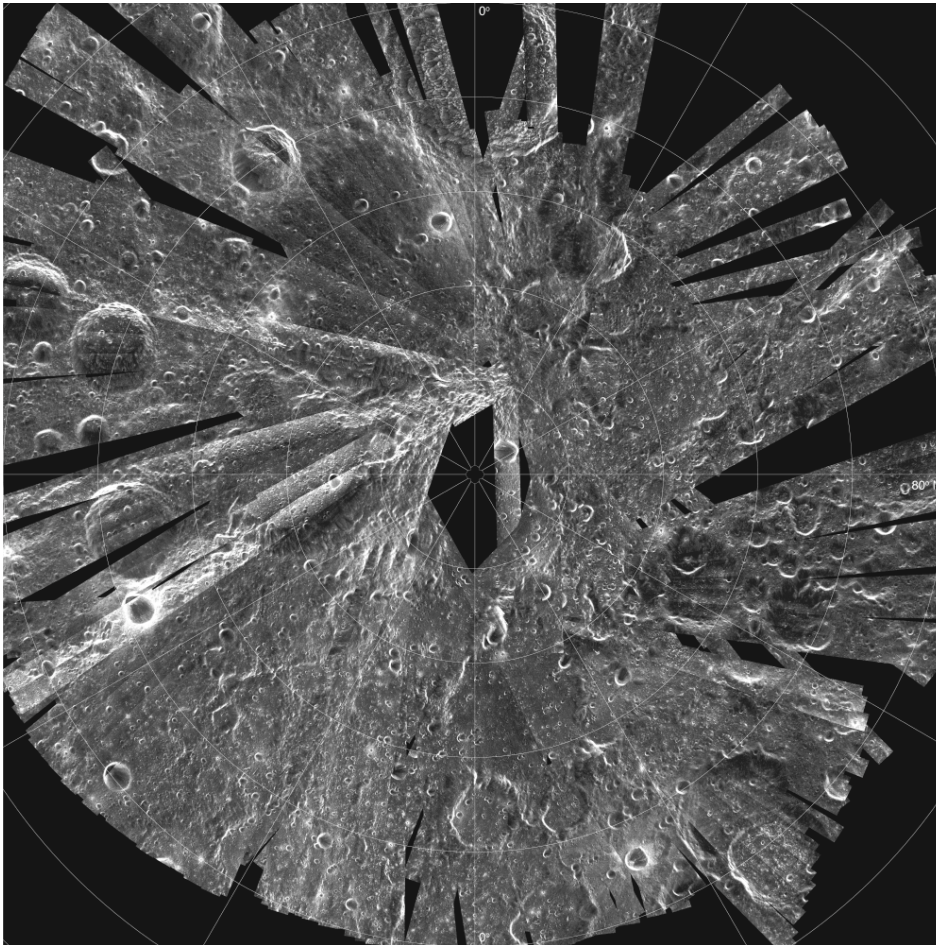


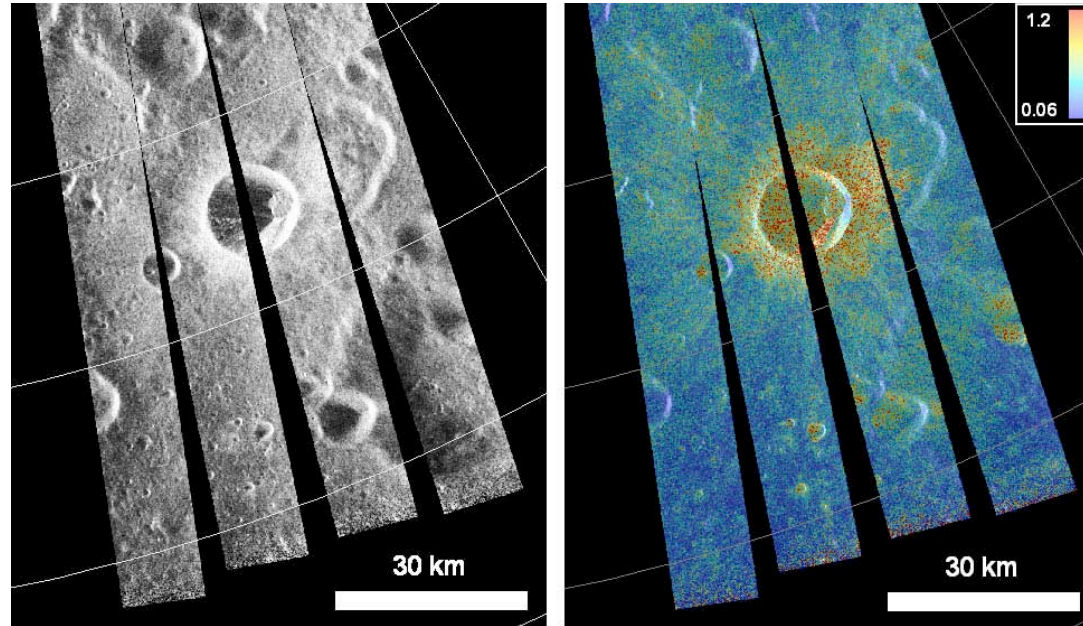
South Polar Mosaic





North Polar Mosaic

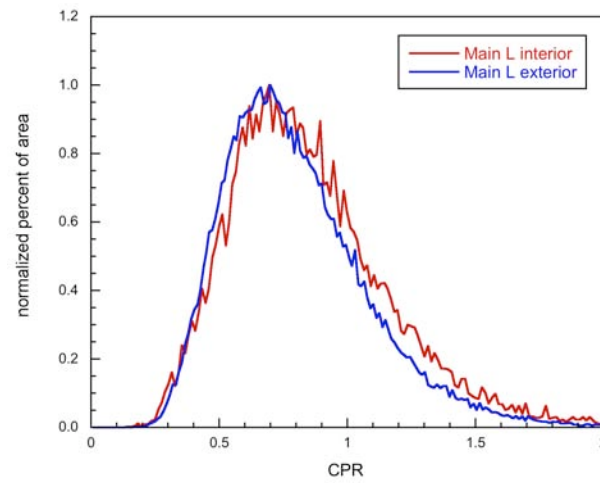


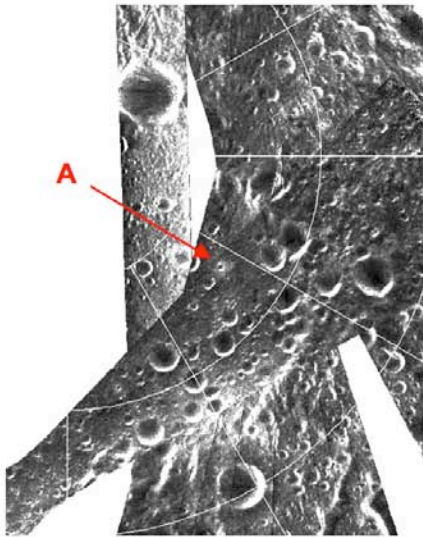


OS SAR image

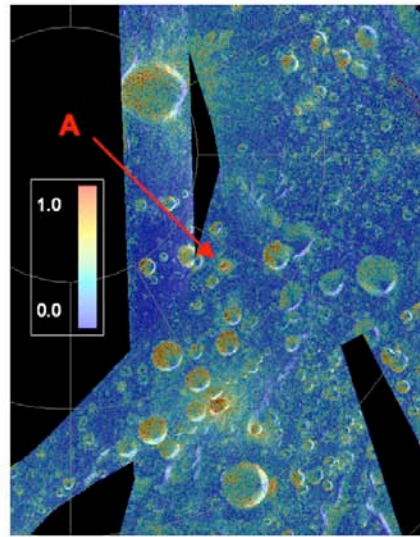
Main L
14 km diameter
81.4° N, 22° E

CPR image

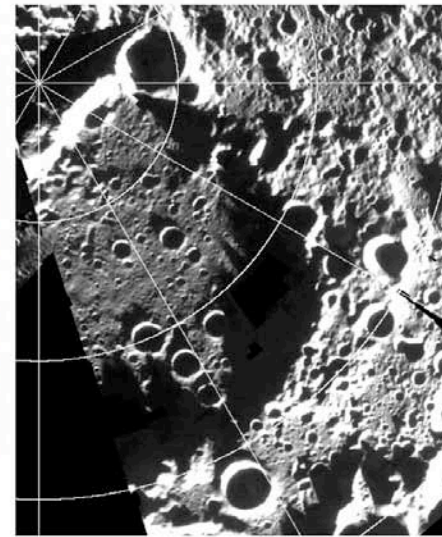




OS SAR mosaic

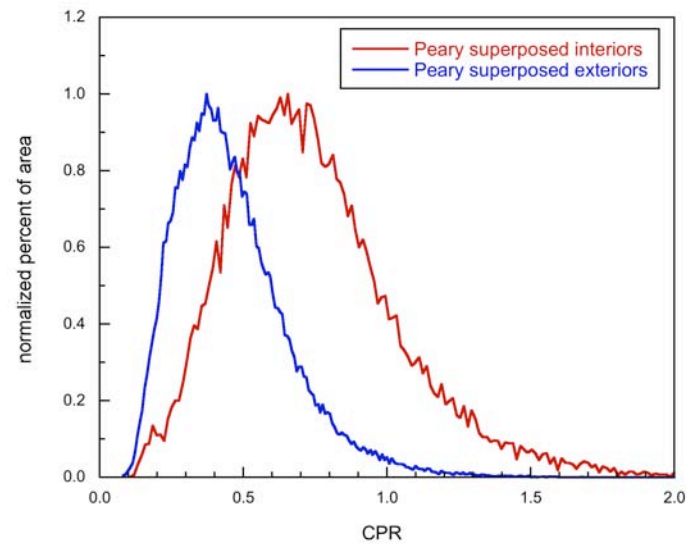


CPR mosaic



Clementine hires mosaic

Floor of Peary
73 km diameter
88.6° N, 33° E

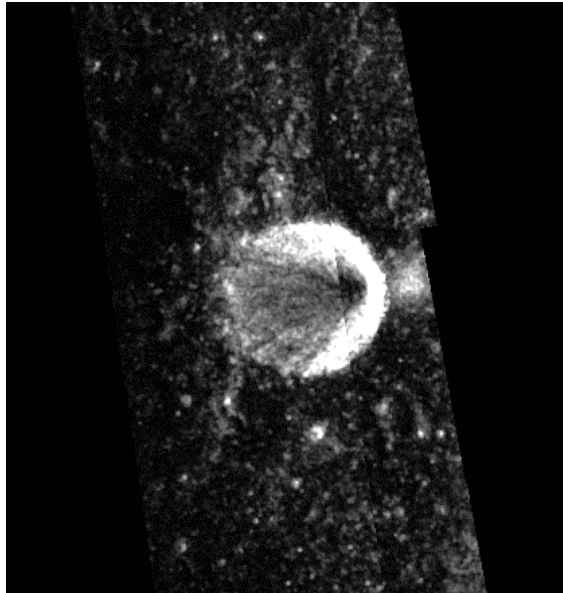




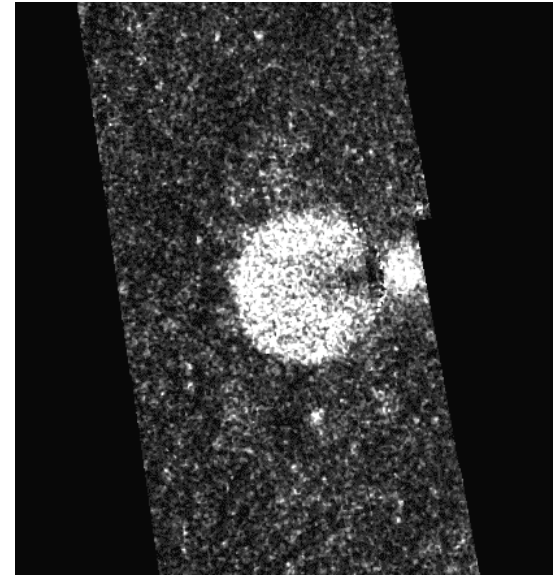
Anomalous polar crater

Rozhdestvensky N, 9 km diameter, 84.3 N, 157 W

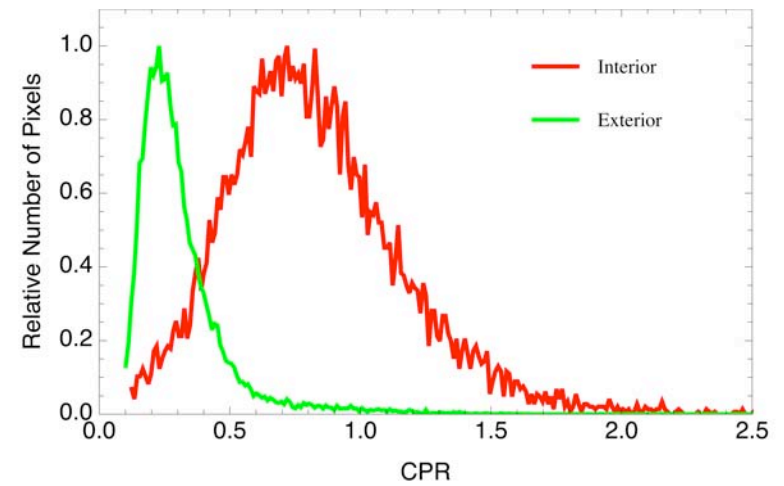
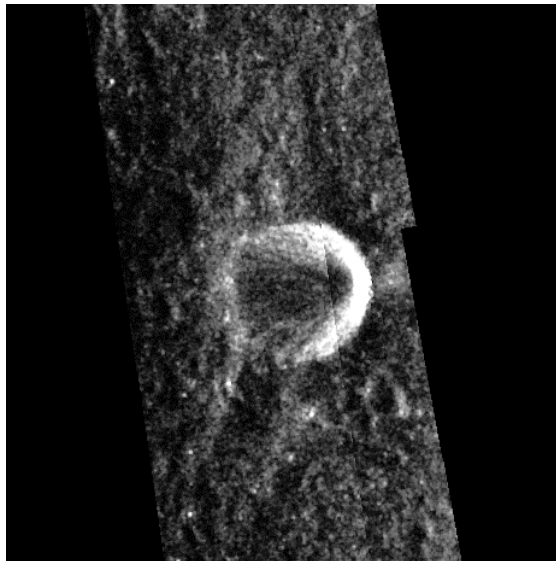
SC



CPR



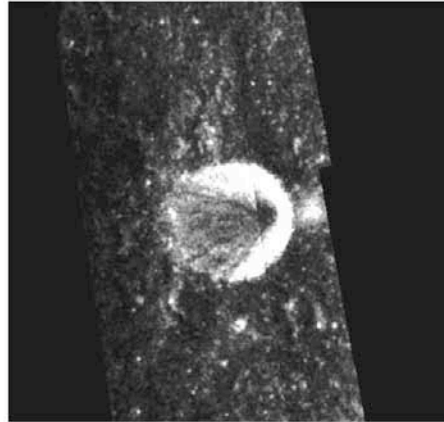
OC



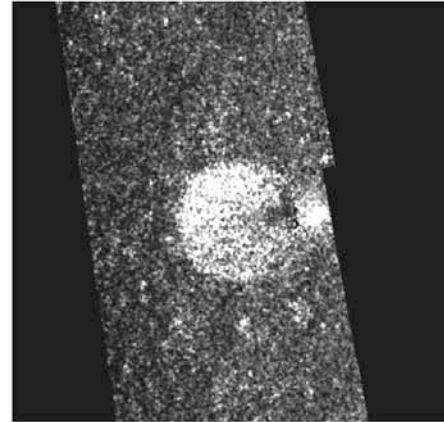


Rozhdestvensky N

SC

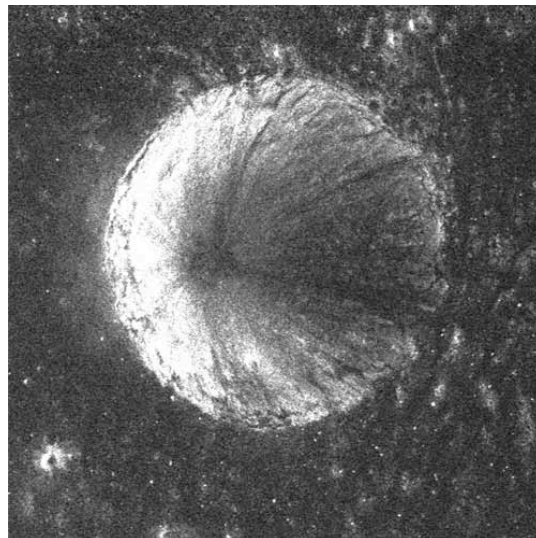


CPR

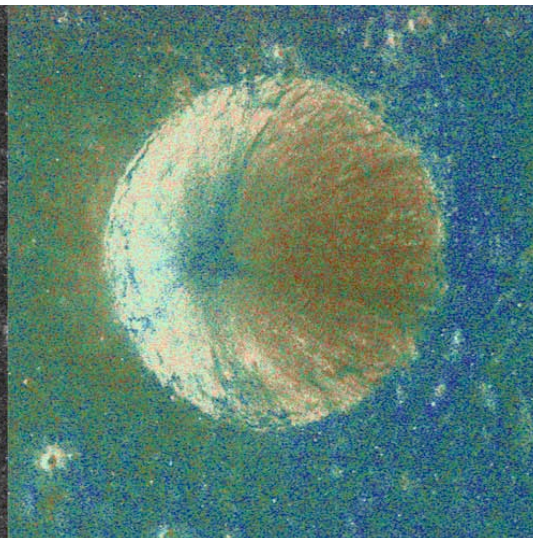


Illumination direction

SC



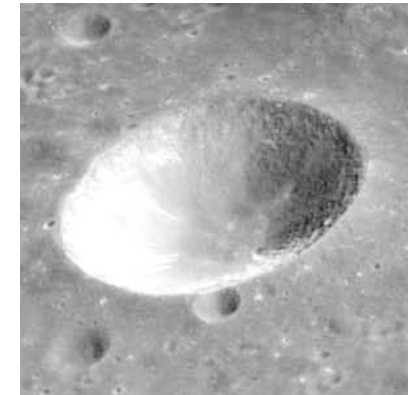
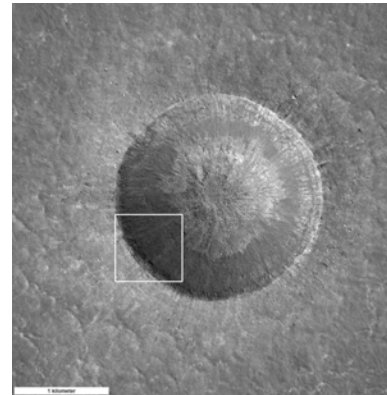
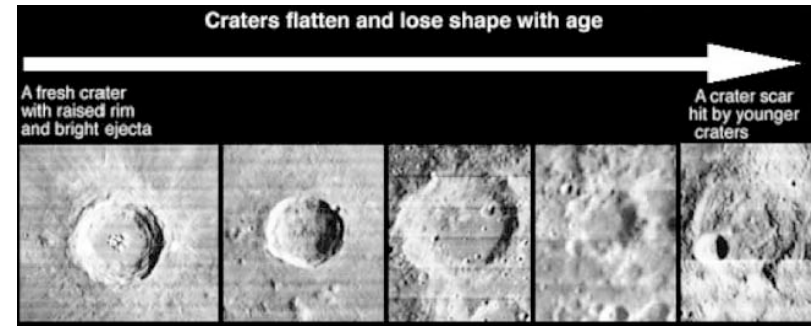
CPR





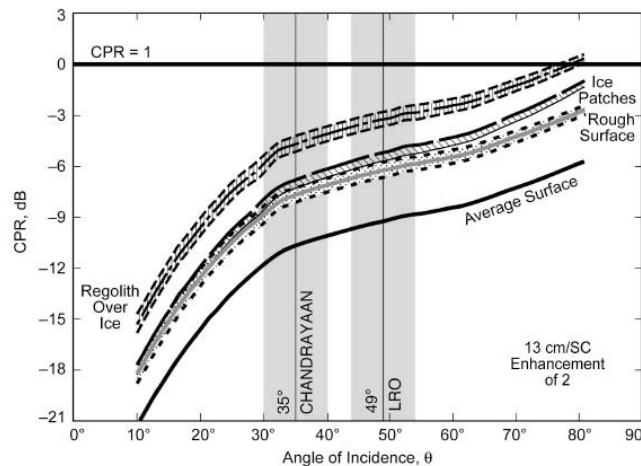
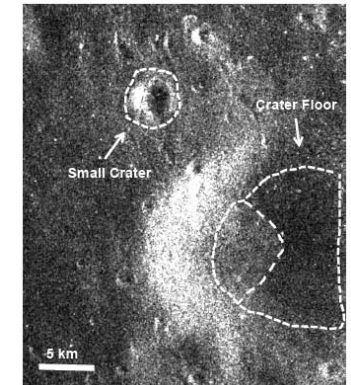
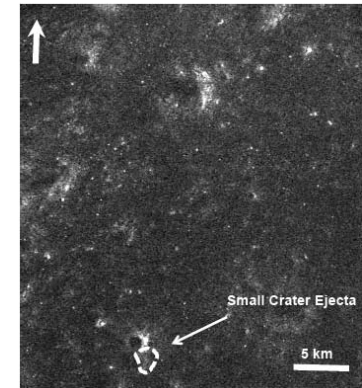
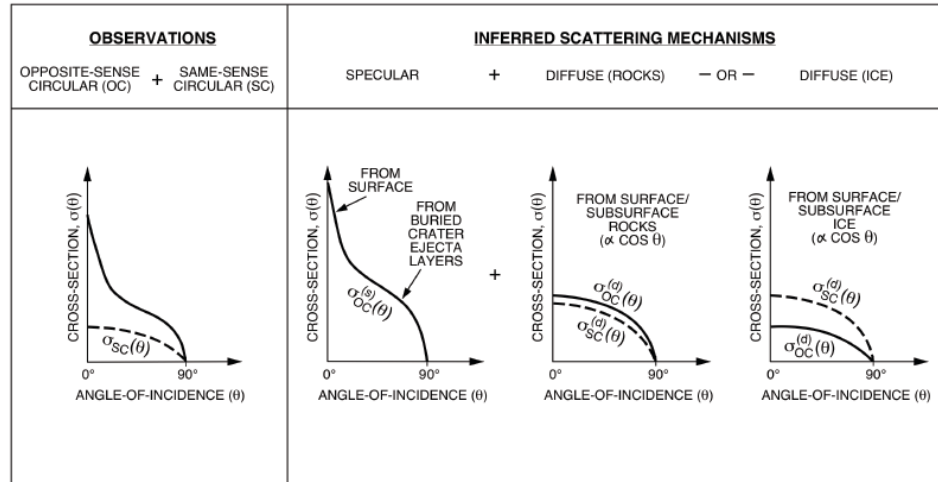
Geological evidence

- Anomalous craters have high CPR inside their rims, but not outside
- Fresh craters have high CPR inside and outside their rims
- As craters age and erode, this surface roughness is lost (rocks buried, eroded, covered by fine material)
- Degradation occurs both inside and outside of the crater rim
- Thus, the high CPR confined inside rims of anomalous craters is probably **not** caused by surface roughness





Modeling scattering from ice and regolith



Separates for Thin Regolith over Ice from Rough Surface

No Separation for Ice Patches from Rough Surfaces

| Site | Small Mid-Latitude Crater Ejecta | Small Polar Crater (88-N) | Mid-Size Polar Crater Floor (88-N) | Mid-Size Polar Crater Bright Debris (88-N) |
|---------------------------------|----------------------------------|------------------------------------------------|------------------------------------|--------------------------------------------|
| Alpha, SC Enhancement | 1.66 | 1.38 | 1.75 | 1.72 |
| Gamma, OC Enhancement | 1.00 | 0.74 | 1.14 | 1.16 |
| CPR-obs = (Alpha*CPR_avg)/Gamma | 0.23 | 0.26 | 0.21 | 0.21 |
| CPR Rough Surface Model | 0.24 | 0.21 | 0.25 | 0.25 |
| CPR Ice Patches Model | 0.27 | 0.23 | 0.29 | 0.28 |
| CPR Thin Regolith over Ice | 0.42 | 0.31 | 0.45 | 0.44 |
| | Matches Rough Surface | Matches Ice Patches and Thin Regolith over Ice | Matches Rough Surface | Matches Rough Surface |



Statistical analysis of high CPR craters

Analyzing all polar craters, fresh and anomalous, to determine statistical properties of the high CPR

All distributions are log-normal

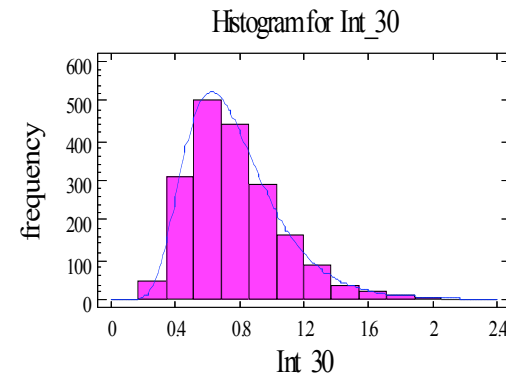
Initial analyses suggested to

Spudis *et al.* (2010) that anomalous crater

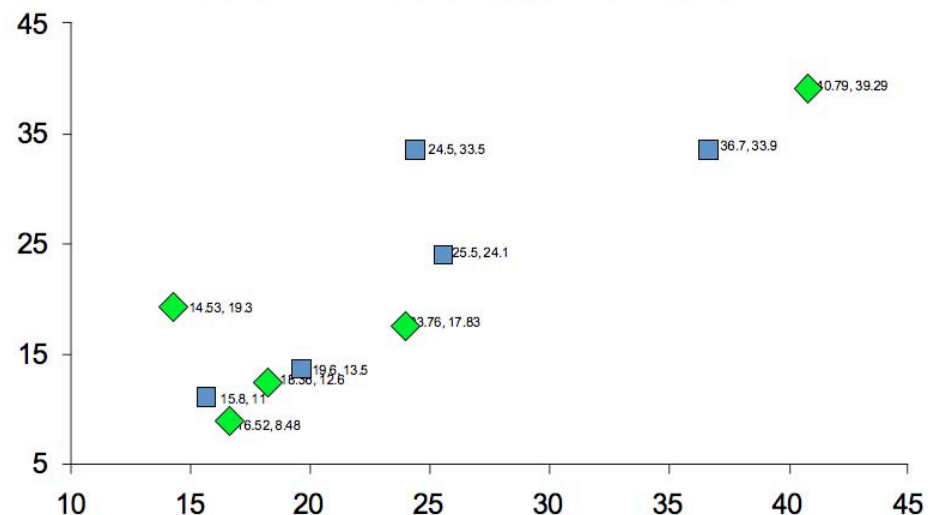
Rozhdestvensky N had CPR distribution distinct from “normal” crater Main L

New analyses confirm and extend this result

Additional work will include both poles, non-polar examples



Skew vs Kurtosis/ANOM vs Fresh

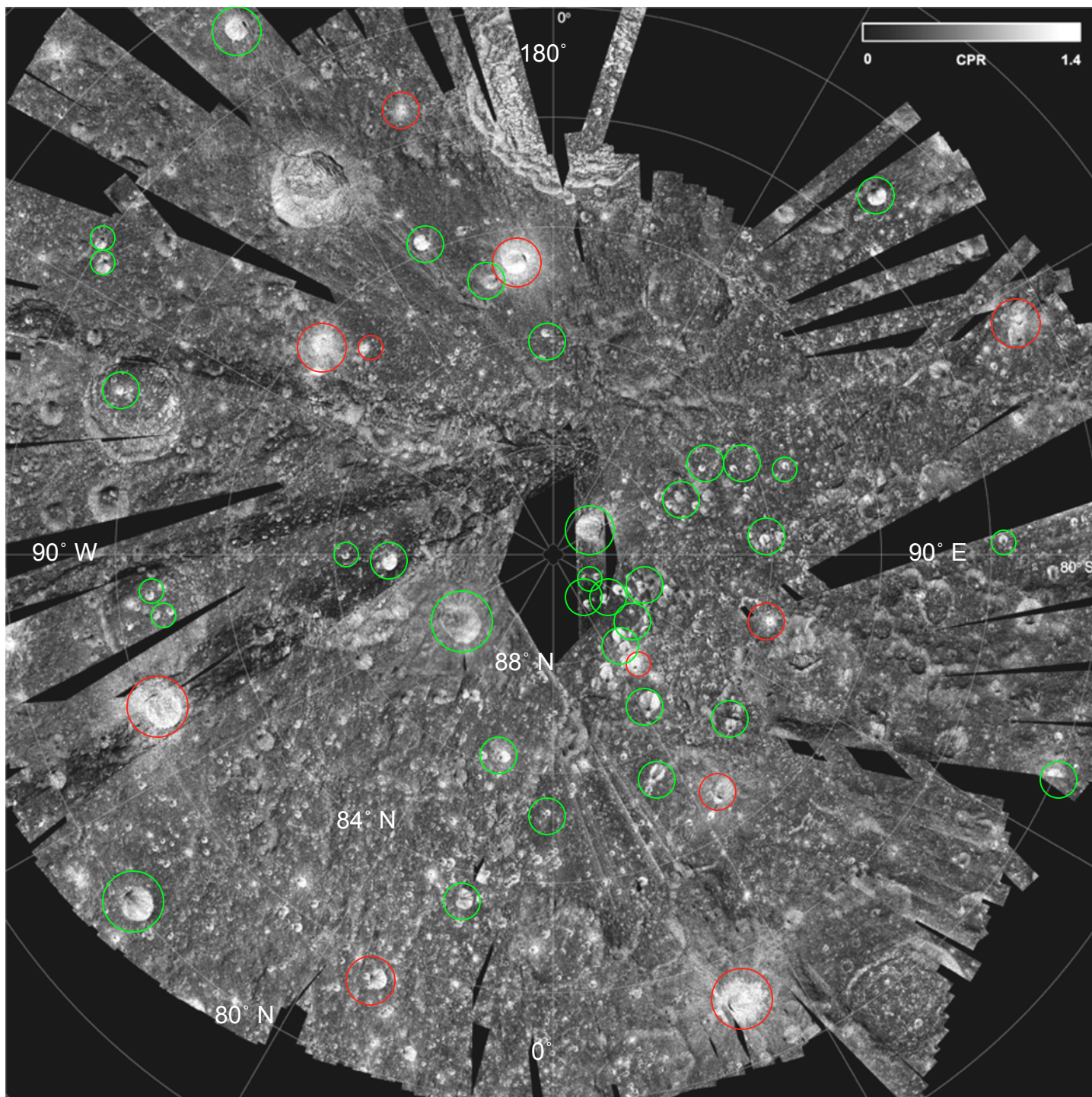




Fresh craters



Anomalous craters

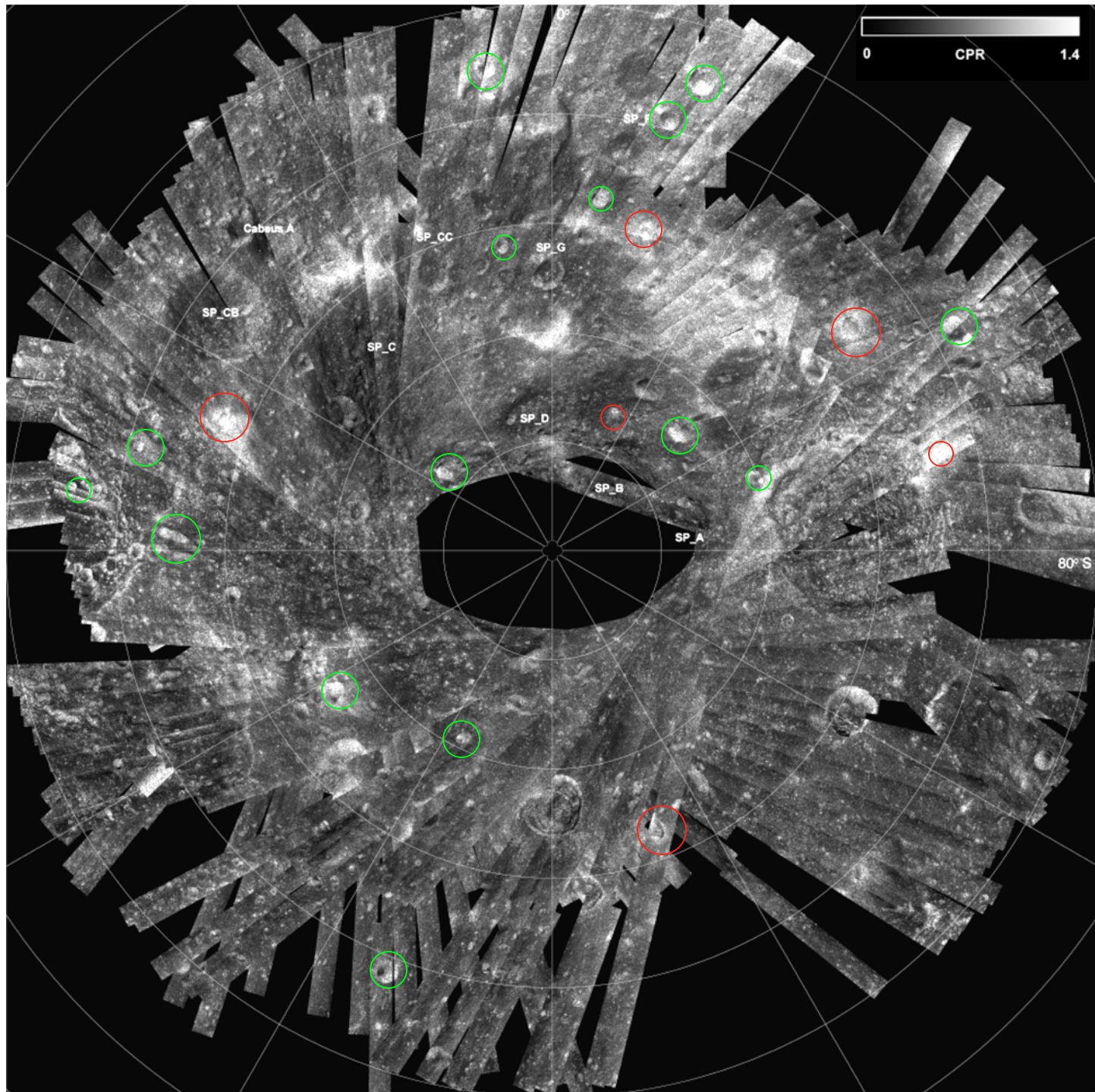




Fresh craters



Anomalous craters

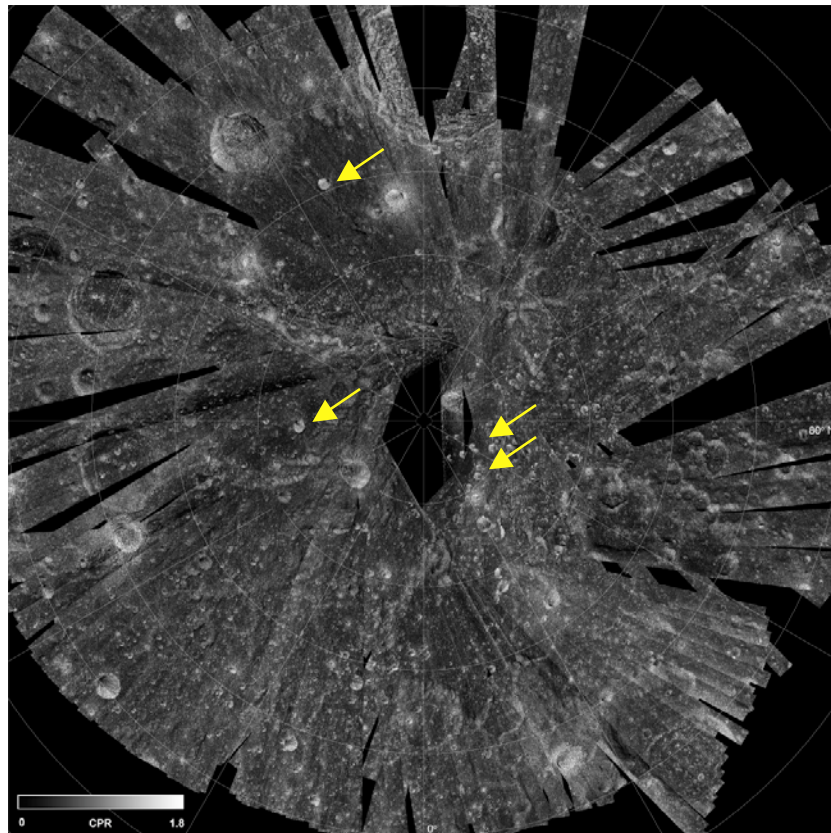




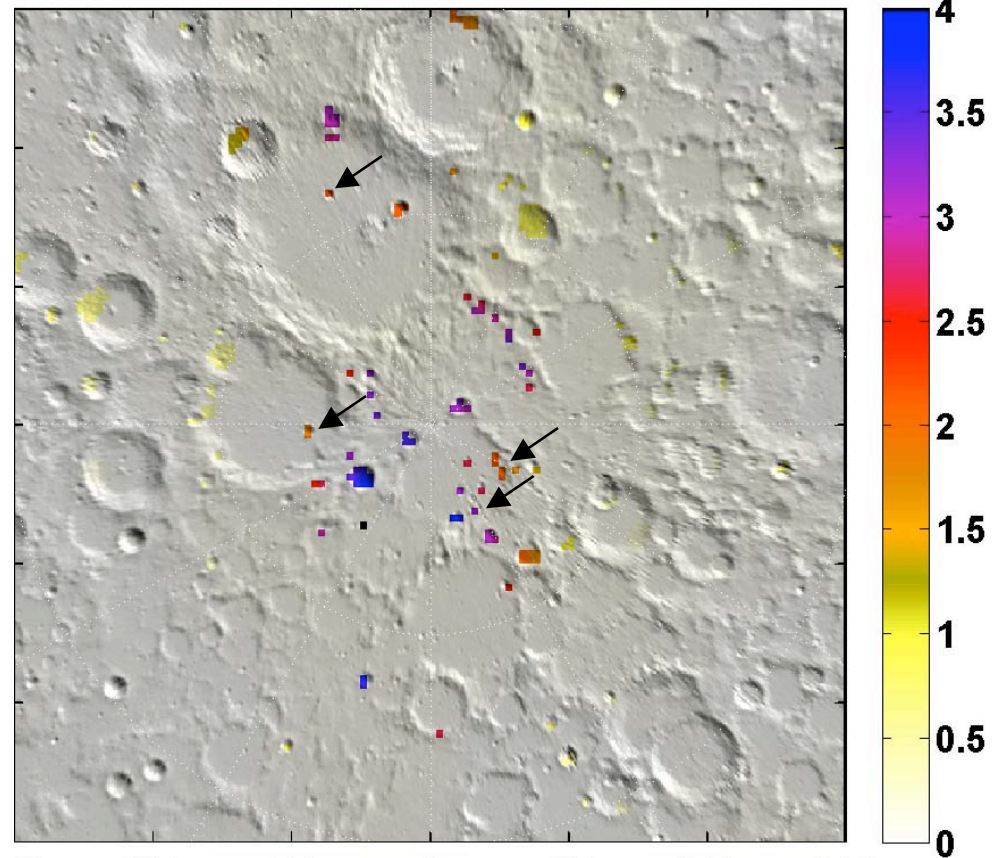
CPR v. Neutron data



Water Equivalent Hydrogen
wt. %



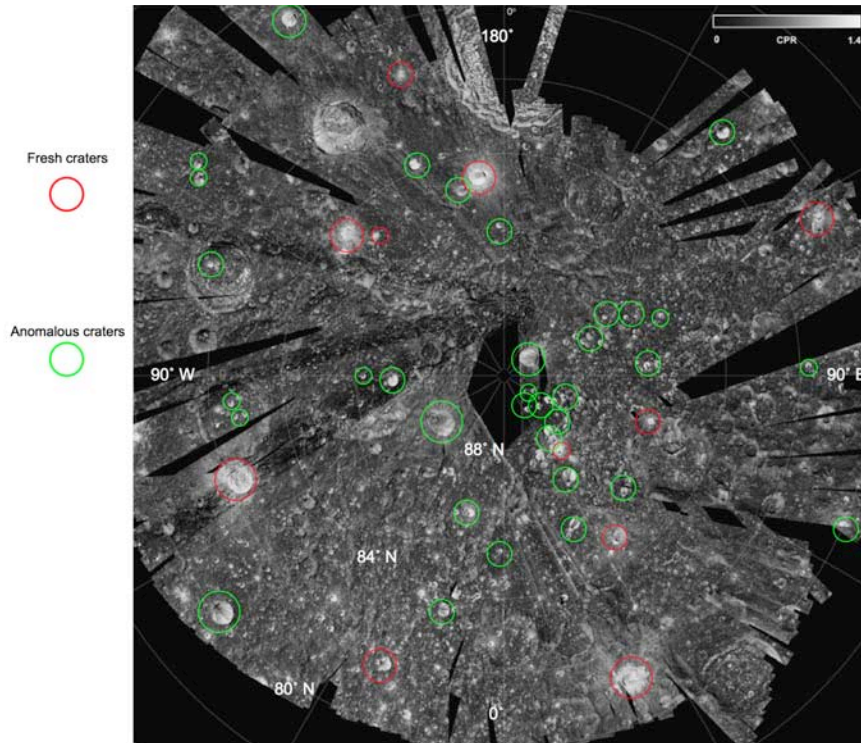
Mini-SAR CPR



LP Neutron Pixon Model



How Much Ice?



| 1 | D (km) | A (km ²) | V (m ³ /m (mT)) |
|----|-----------------------------|----------------------|----------------------------|
| 2 | 12 | 113.04 | 24000000 |
| 3 | 8 | 50.24 | 16000000 |
| 4 | 7 | 38.465 | 14000000 |
| 5 | 5 | 19.625 | 10000000 |
| 6 | 6 | 28.26 | 12000000 |
| 7 | 8 | 50.24 | 16000000 |
| 8 | 3 | 7.065 | 6000000 |
| 9 | 5 | 19.625 | 10000000 |
| 10 | 4 | 12.56 | 8000000 |
| 11 | 4 | 12.56 | 8000000 |
| 12 | 8 | 50.24 | 16000000 |
| 13 | 21 | 346.185 | 42000000 |
| 14 | 18 | 254.34 | 36000000 |
| 15 | 7 | 38.465 | 14000000 |
| 16 | 12 | 113.04 | 24000000 |
| 17 | 3 | 7.065 | 6000000 |
| 18 | 8 | 50.24 | 16000000 |
| 19 | 6 | 28.26 | 12000000 |
| 20 | 11 | 94.985 | 22000000 |
| 21 | 6 | 28.26 | 12000000 |
| 22 | 4 | 12.56 | 8000000 |
| 23 | 5 | 19.625 | 10000000 |
| 24 | 4 | 12.56 | 8000000 |
| 25 | 6 | 28.26 | 12000000 |
| 26 | 4 | 12.56 | 8000000 |
| 27 | 3 | 7.065 | 6000000 |
| 28 | 3 | 7.065 | 6000000 |
| 29 | 8 | 50.24 | 16000000 |
| 30 | 17 | 226.865 | 34000000 |
| 31 | 4 | 12.56 | 8000000 |
| 32 | 34 | 907.46 | 68000000 |
| 33 | 4 | 12.56 | 8000000 |
| 34 | 6 | 28.26 | 12000000 |
| 35 | 5 | 19.625 | 10000000 |
| 36 | 4 | 12.56 | 8000000 |
| 37 | 4 | 12.56 | 8000000 |
| 38 | 3 | 7.065 | 6000000 |
| 39 | 8 | 50.24 | 16000000 |
| 40 | 5 | 19.625 | 10000000 |
| 41 | 11 | 94.985 | 22000000 |
| 42 | | | |
| 43 | Total ice (m ³) | | 608000000 |
| 44 | | | |
| 45 | Total reg (m ³) | | 5.652E+11 |
| 46 | | | |
| 47 | Concentration | | 0.001075725 |

Observed high CPR area in shadowed craters x 10(λ) thickness
 Total N. Polar ice $\sim 6 \times 10^8 \text{ m}^3 = 600 \text{ million mT}$
 Average fuel mass in Shuttle ET = 735 mT (735,000 kg)
 Enough LH_2/LO_2 for one Shuttle launch equivalent *per day* for more than 2200 years



The Lunar Hydrosphere

The Five Flavors of Lunar Water

Water is or was in the lunar interior (as a *minor* component; 250-700 ppm)

Water from deep mantle (> 400 km depth) component of volatiles driving lunar pyroclastic eruptions

Water and OH molecules present at latitudes > 65° at both poles

Present as adsorbed monolayer and/or bound in mineral structures

Increasing concentration with increasing latitude (~800 ppm and *greater*)

Temporally variable; preferentially located in cooler locales (it's moving)

Exospheric water is present in space above the south pole

MIP mass spectrometer measured $\sim 10^{-7}$ torr partial pressure H_2O

Water ice is admixed into regolith in polar regions

LCROSS site (floor of Cabeus) is 5-10 wt.% water; both ice particles and water vapor ejected during impact

Other cometary volatiles are present (e.g., carbon dioxide, methane, sulfur dioxide, methanol, ethanol)

Concentrations vary laterally, vertically; “fluffy” physical nature

Thick (~2 m), “pure” water ice is found in some permanently shadowed craters near the poles

High CPR materials in over 40 craters (3-12 km dia.) near north pole

Suggest over 600 million metric tonnes of “pure” water ice; reserves of ice mixed with dirt are much greater



Summary

Mini-SAR successfully mapped more than 90% of both polar areas
Thirteen non-polar areas analyzed; results consistent with previous
S-band radar mapping from Earth

Areas of high CPR have been identified:

- Some high CPR is clearly associated with surface roughness (e.g.,
Main L ejecta blanket)

- Some deposits (e.g., near north pole on floor of Peary) show high
CPR and are restricted to the *interior* of craters; these features are
in permanent darkness.

- Statistical analysis suggests that these features constitute a distinct
population from normal, fresh crater high-CPR features

Anomalous craters are found at both poles and correlate with Pixon
model reconstructions of LP neutron data and areas of low
surface temperature revealed by DIVINER

These anomalous deposits are probably water ice. Over 600
million m³ are present in vicinity of north pole in this form



Mini-RF high resolution SAR of polar areas

